**Article:**

Schirru, M., Mills, R., Dwyer-Joyce, R. et al. (2 more authors) (2015) Viscosity Measurement in a Lubricant Film Using an Ultrasonically Resonating Matching Layer. Tribology Letters, 60 (42). ISSN 1023-8883

https://doi.org/10.1007/s11249-015-0619-x

# Viscosity measurement in a lubricant film using an ultrasonically resonating matching layer

**M. Schirru[1], R. Mills [1], R. Dwyer-Joyce[1], O. Smith[2] and M. Sutton[2]**

1. **The Leonardo Centre for Tribology**
2. **The Lubrizol Corporation**

## Abstract

A novel ultrasonic viscometer intended for in-situ applications in lubricated components is presented. The concept is based on the reflection of a shear wave at a solid-liquid boundary that depends on the viscosity of the liquid and the acoustic properties of the solid. Very little ultrasound energy can propagate into the oil at a metal-oil interface because the acoustic mismatch is great, and this leads to large measurement errors. The method described in this paper overcomes this limitation by placing a thin intermediate matching layer between the metal and the lubricant. Results obtained with this technique are in excellent agreement with expected values from conventional viscometers when Newtonian mineral oils are analysed. When complex non-Newtonian mixtures are tested the viscosity measurement is frequency dependent. At high ultrasonic frequencies, over 1 MHz, it is possible to shear only the base oil, while to obtain the viscosity of the mixture it is necessary to choose a lower excitation frequency to match the dispersed polymer relaxation time.

## 1 Introduction

Conventional viscometers cannot reproduce the operating conditions in an engine bearing. The temperature, pressure, shear rate, lubricant response, contamination and degradation are all unique features to the operating environment.

An alternative to mechanical viscometers used to shear a liquid are shear polarised ultrasonic waves. Early work dedicated to this method was performed by Mason [1] who correlated reflected energy from a piezoelectric (PZT) quartz crystal to the viscosity of a liquid sample in contact with the transducer. Since then, other authors have used reflectance methods to study viscosity in a bulk fluid [2] and in industrial processes where the fluid involved could be considered Newtonian [3]: for example diagnostic analysis of coal combustion processes [4] or for characterization of resins in an autoclave [5]. Most ultrasonic viscometry studies assume that the liquid is Newtonian [6, 7, 8]. A first attempt to study complex lubricants and elastohydrodynamic lubrication (EHL) by means of ultrasound waves was made by Lamb and Barlow [9, 10]. These researchers developed models for the analysis of non-linear fluid behaviour by taking into account particle relaxation time.

Despite the improvements in ultrasonic techniques, direct viscosity measurement in components such as engine bearings has not been possible. Most engine bearing materials are metallic and so are highly acoustically mismatched with the lubricant. This means that very little of the ultrasonic wave propagates into the liquid and measurements of reflection are subject to significant scatter.

It is the aim of this work to develop a viscometry technique that can be used in engines in-situ. A methodology to analyse mineral oils and engine lubricants by means of a novel ultrasound matching layer technique is presented. A thin layer of suitable acoustical properties is interleaved between the solid and the oil sample to allow a better sound transmission across the interface and so an increase in the measurement sensitivity.

## 2 Reflection of shear waves from a thin liquid film

When an ultrasonic shear polarized wave strikes the boundary between a solid-liquid interface the ultrasonic energy is partly transmitted and dissipated in the fluid, and partly reflected back to the ultrasonic source as an echo wave (see Figure 1a). The amount of ultrasonic energy reflected from the solid liquid interface is quantified in form of a reflection coefficient, $R$:

$$R = \frac{z_s - z_l}{z_s + z_l} \tag{1}$$

Where $z_s$ is the acoustic impedance of the solid and $z_l$ is the acoustic impedance of the liquid layer and $R$ is a complex quantity that can be defined in terms of modulus and phase by:

$$R = |R|e^{-i\omega\theta} \tag{2}$$

Where $|R|$ is the reflection coefficient modulus and $\theta$ is the reflection coefficient phase. The acoustic impedance of the solid is a real quantity defined as:

$$z_s = \rho_s c \tag{3}$$

Where $\rho_s$ is the density of the solid medium, while $c$ is the shear speed of sound in the solid. The acoustic impedance of the liquid is a function of the density, $\rho_l$ and shear modulus:

$$z_l = \sqrt{\rho_l G} \tag{4}$$

$G$ is the complex shear modulus, given by $G = G' + iG''$ where $G'$ is the storage modulus and $G''$ is the loss modulus. The complex shear modulus can be correlated to the reflection coefficient by combining equation (1) and equation (4) as:

$$R = \frac{z_s - \sqrt{\rho_l G' + iG''}}{z_s + \sqrt{\rho_l G' + iG''}} \tag{5}$$

For a purely Newtonian fluid $G'$=0 and the viscosity can be related to the loss modulus by [11]:

$$G'' = \omega\eta \tag{6}$$

Where $\omega = 2\pi f$ is the angular frequency.

Combining equation (5) and equation (6) the viscosity is [12]:

$$\eta = \frac{{z_s}^2}{\rho_l \omega}\left[\frac{4|R|(1-|R|^2)sin\theta}{1+|R|^2+2|R|cos\theta}\right] \tag{7}$$

Such a model is valid only for perfectly Newtonian fluids. In previous work [13], a method to take into account of the viscoelasticity the oils was proposed. This model was implemented by means of the Maxwell model mechanical analogy:

$$\eta = \frac{{z_s}^2}{\rho_l \omega}\left(\frac{4|R|(1-|R|^2)sin\theta}{(1+|R|^2+2|R|cos\theta)^2}\right)(1+\omega^2\tau^2) \tag{8}$$

Where $\tau$ is the relaxation time and takes into account the viscoelastic effects. When the fluid is Newtonian relaxation effects are negligible and $\tau$ tends to *0*. In that case equation (8) reduces to equation (7).

Ultrasonic shear waves can propagate through fluids, but only for very short distances because the wave dissipates energy quickly. The distance travelled by a shear wave in a fluid before being completely dissipated is called the penetration depth, $\delta$ which can be calculated as [14]:

$$\delta = \sqrt{\frac{\eta}{\pi f \rho_l}} \tag{9}$$

From equation (9), if $\eta$ is of 0.01 Pas, $f$ is 5 MHz and $\rho_l$ is of 800 $\mathrm{kg\,m^{-3}}$ then the penetration depth will be less than 1 µm. Common lubricated layer thickness ranges from 5 to 80 µm in hydrodynamic journal bearings. This means that a lubricated layer behaves like a semi-infinite space because the ultrasonic wave does not propagate throughout the whole fluid layer, as shown in Figure(1).

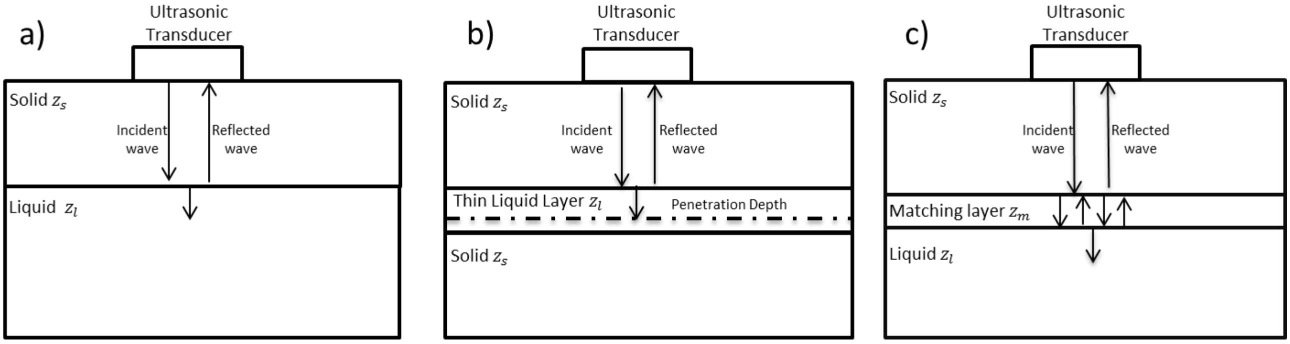

**Figure 1: a) Shear ultrasound transmission and reflection from a solid-liquid boundary, (b) Shear ultrasound transmission and reflection from a solid-liquid-solid system, (c) Shear ultrasound transmission and reflection from a solid-matching layer-liquid system.**

## 3 Matching layer methodology

Inspection of equation (1) shows that when the acoustic impedance of the solid is much higher than the acoustic impedance of the liquid, the reflection coefficient tends to one. This is the case for metal-oil interfaces and so the common reflectance measurement is highly insensitive to the oil properties. Because most engine bearings are metallic, this practically precludes such a measurement method.

To overcome this limitation, a quarter wavelength matching layer is used to increase the acoustic response, as shown in Figure (1c). This method is commonly used in the production of ultrasonic immersion transducers or non-contact probes, where a quarter-wavelength-thick layer bonded to the transducer is used to acoustically couple the piezoelectric element to water or air [15].

The ultrasonic waves produced by the transducer travel to the matching layer. Figure (2) schematically shows the resonance phenomenon. Inside this layer the waves superimpose in-phase, producing a larger resultant. Simultaneously the reflected wave from the layer cancels out the incident wave. The overall effect is to greatly increase the transmitted energy into the oil and reduce the reflected energy. In this way the signal to noise ratio (SNR) and sensitivity to lubricant viscosity is improved.

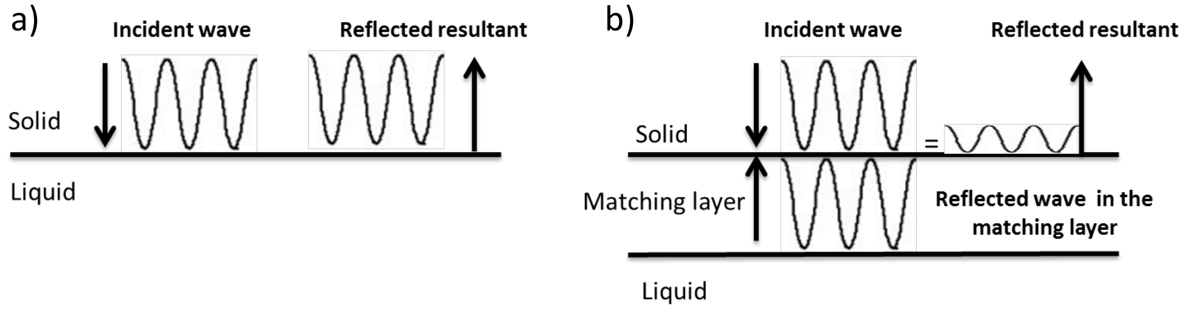

**Figure 2: (a) Shear wave total reflection from a solid-liquid boundary: the wave is almost completely reflected (b) Ultrasound wave resonance in the matching layer: the attenuated reflected resultant is shown.**

The optimum matching layer is designed to minimise ultrasonic reflection at the solid-matching layer-liquid boundaries. The reflection coefficient in a three-layered system is given by [16]:

$$R = 1 - \frac{4}{\left[2 + \left(\frac{z_l}{z_s} + \frac{z_s}{z_l}\right) cos^2(k_m t) + \left(\frac{{z_m}^2}{z_s z_l} + \frac{z_s z_l}{{z_m}^2}\right) sin^2(k_m t_m)\right]} \qquad (10)$$

Where $z_m$ is the matching layer acoustic impedance, $t_m$ is the matching layer thickness and $k_m = \frac{2\pi}{\lambda_m}$ is the matching layer wave number, where $\lambda_m$ is the wavelength in the matching layer. The matching layer thickness is chosen to be equal to a multiple of a quarter of the wavelength in the layer:

$$t_m = \frac{nc_m}{4f} \tag{11}$$

Where *n* is a natural integer. If equation (11) in inserted in equation (10) then $cos^2(k_m t) = \cos(\pi/2) = 0$ and $sin^2(k_m t) = \sin(\pi/2) = 1$ and this leads to the following simplification for equation (10):

$$R = 1 - \frac{4z_s z_l}{\left(z_m + \frac{z_s z_l}{z_m}\right)^2} \tag{12}$$

Solving equation (12) for minimum reflection (i.e., *R*=0) gives a matching layer acoustic impedance of:

$$z_m = \sqrt{z_s z_l} \tag{13}$$

The ideal matching layer is defined by equations (11) and (13). In equation (13), the value of $z_m$ is not constant, but depends on the fluid being studied. This is because $z_l$ is a function of frequency and viscosity according to equation (4). For the case of a Newtonian fluid combining equations (4), (6) and (13) gives the required matching layer impedance as:

$$z_m = \sqrt{z_s\sqrt{\rho_l 2\pi f \eta}} \tag{14}$$

Equation (14) shows that the optimum matching layer impedance is a function of the excitation frequency. Therefore, as well as selecting a layer to match the material properties, it is important to match the transducer frequency bandwidth. Figure (3) shows the optimum matching material acoustic impedance calculated with equation (14) in case of a fluid of 0.25 Pas viscosity, density of 900 $\mathrm{kgm^{-3}}$ and for transducer frequency varying from 100 kHz to 10 MHz for both aluminium, steel or tungsten carbide solid body. For example, when measuring at 5 MHz on a steel bearing the matching layer material should have an acoustic impedance of 1.3 MRayl. It can be noticed that the acoustic properties of the matching layer change considerably from low to high ultrasonic frequencies.

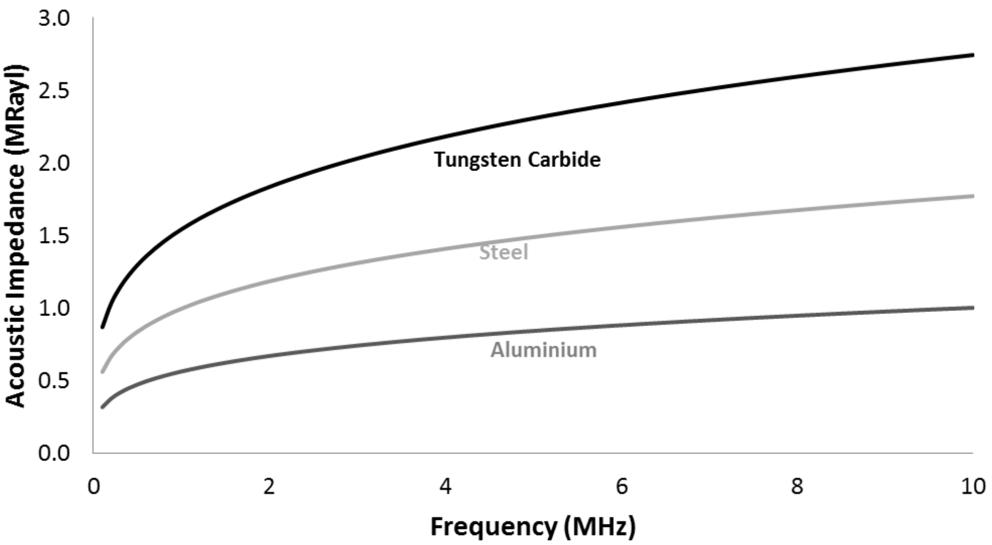

**Figure 3: Optimum matching layer acoustic impedance for bearing materials of aluminium, steel and tungsten carbide coupled with an oil of viscosity 0.25 Pas and density 900 $\mathrm{kgm}^{-3}$ over a range of ultrasonic frequencies.**

The 'ideal' values of the matching layer impedance and thickness (i.e., values that lead to *R*=0) are given by equations (11) and (14). Figure (4) shows the effect of deviation from the ideal matching layer acoustic impedance and thickness on *R* calculated using equation (10). The results are calculated for the transducer frequency of 5 MHz and for a lubricant with viscosity of 0.25 Pas and density of 900 kgm$^{-3}$. Sensitive ultrasonic measurements are possible when *R*<0.9; for values greater than this the reflected signal is too close in magnitude to the incident signal and measurements suffer from noise. The plot shows the acceptable combinations of matching layer thickness. So polyimide matching layers are suitable for all three bearing metals; whereas a lead-based Babbitt is on the limit for steel.

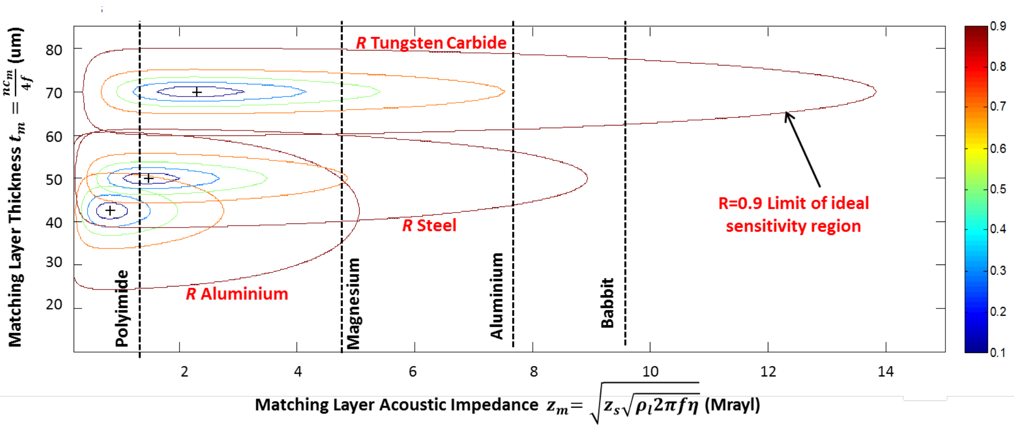

**Figure 4: Reflection coefficient sensitivity to matching layer acoustic impedance and thickness in case of solid body of aluminium or tungsten and oil with viscosity of 0.25 Pas and density of 900 $\mathrm{kgm}^{-3}$.**

As an example, the selection of a matching layer for an aluminium bearing material (shear acoustic impedance of 8 MRayl) is analysed. The first step is to calculate the acoustic impedance of the matching material. Application of equation (13) gives a value of matching acoustic impedance of 0.9 MRayl. This impedance value fits most plastics, polymers and epoxies. Among all the possible materials polyimide is chosen because the nominal shear acoustic impedance is close to the ideal one at 1.4 MRayl. Polyimide has already been used as a matching layer for air and immersion probes; also it comes in thin layers easy to bond to any surface and is resistant to high temperatures (the melting point is of around 300 °C). Once the matching material is chosen, the value of shear speed of sound is inserted in equation (11) to obtain the value of the matching layer thickness by setting $f$=5 MHz and $c_m$= 900 m/s then the thickness of the layer is 45 μm. Figure (5) shows the reflection coefficient for an aluminium-oil boundary both with (equation 10) and without (equation 1) for a desired resonance frequency of 5 MHz. The graph shows that with the application of the matching layer technique different fluid viscosities are much better discriminated at the resonance frequency compared to the common reflectance methodology. Figure (4) shows, also, that the theoretical reflection coefficient for the liquid analysed in the previous example is between 0.7 and 0.8 when the solid is steel and the matching layer is aluminium or babbit. Therefore, this technique can be used in coated components such as steel shell bearing with babbit or alumina based coatings. The expected reflection coefficient from lubricants in contact with these matched materials is, in fact, below the maximum sensitivity threshold of 0.9.

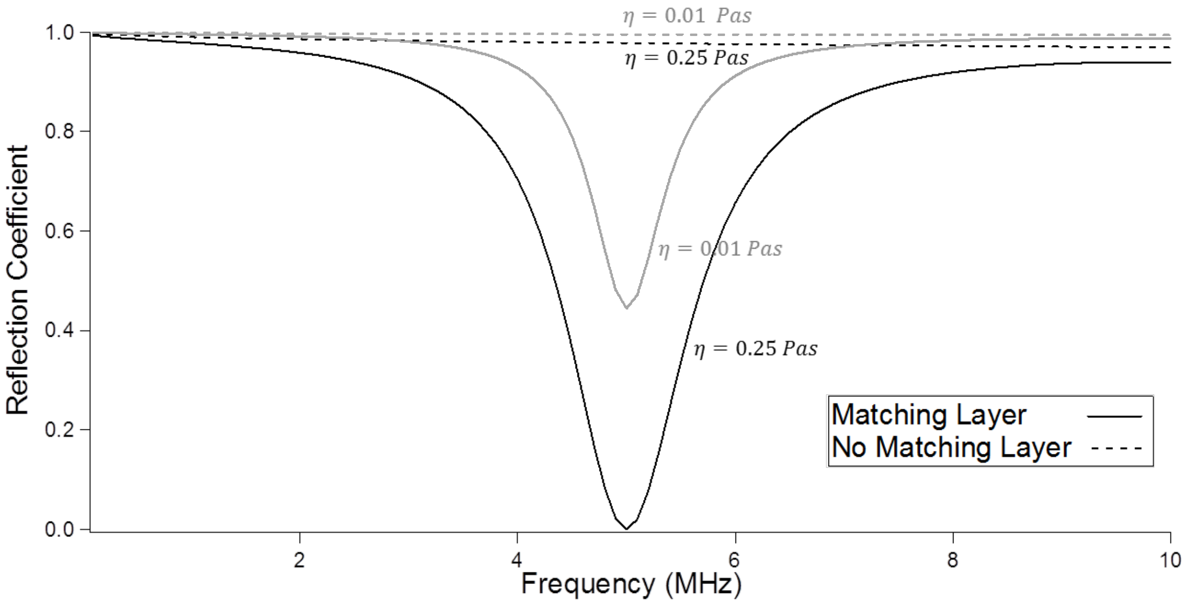

**Figure 5: Reflection coefficient for different fluid viscosity versus frequency with and without matching layer.**

# 4 Measurement Apparatus

## 4.1 Instrumentation

Figure (6) schematically shows the measurement instrumentation. A pair of ultrasonic piezoelectric (PZT) shear mode transducers with a centre frequency of 10 MHz operate in pitch-catch mode. The PZTs are ceramic plates of lead-metaniobiate wrapped in nickel-gold electrodes. One transducer produces the ultrasonic wave (transmitter) and the second one receives the echo wave (receiver). The pulser is excited by a signal produced by an arbitrary waveform function generator (TTI TG5011). Once excited by the electric signal, the pulser vibrates, emitting an ultrasonic wave that propagates through the solid until it is incident on the solid-liquid interface where part of the wave is transmitted and part is reflected back. The reflected signal is received by the receiver sensor and the signal is recorded on an oscilloscope (LeCroy LT342) with a sampling capacity of 500 Ms/s, continuously analysed, and stored in real time using an acquisition interface written in LabView™.

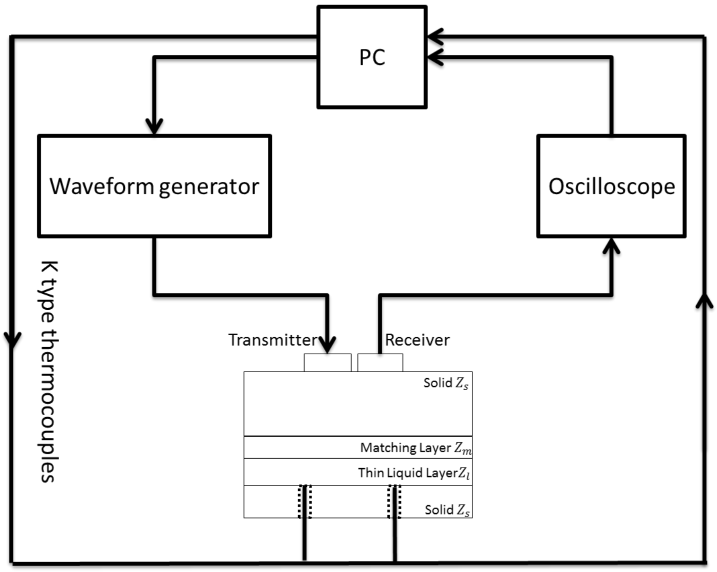

**Figure 6: Schematic diagram of the measurement apparatus.**

## 4.2 Test cell and matching layer

Figure (7) shows the ultrasonic test cell that consists of an aluminium plate 20-mm thick with the ultrasonic transducers bonded underneath. A top solid plate is used to enclose the oil sample in a thin film setup and has holes that allow positioning K-type thermocouples in direct contact with the fluid. Figure (7a) shows the 50 μm polyimide matching layer bonded on the aluminium surface. The choice of the matching layer is based on equations (9) and (11) and is described in details in section 3.

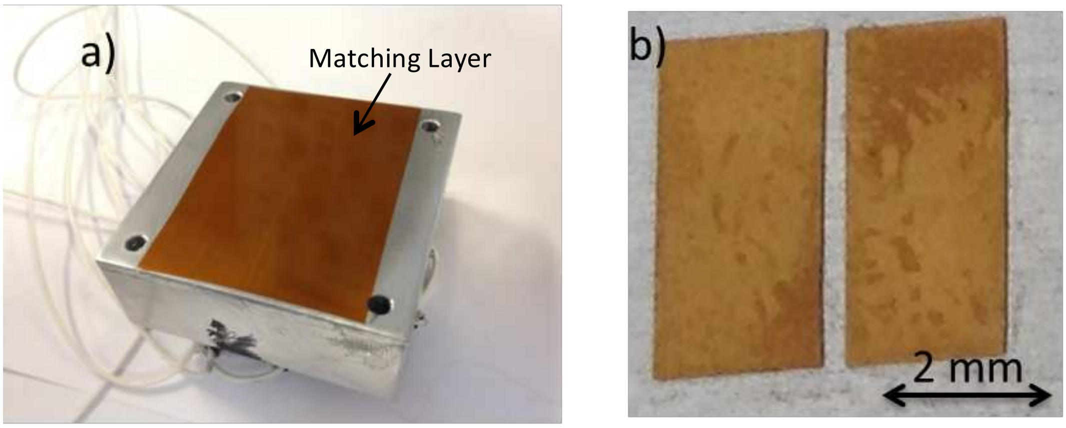

**Figure 7: a) Ultrasonic test cell. (b) Ultrasonic transducers.**

### 4.3 Samples tested

A selection of Cannon™ standard viscosity mineral oils and engine lubricants were tested. Table 1 gives the viscosity data for the samples tested. The Cannon™ standard viscosity oils are Newtonian mineral hydrocarbon base oils tested following the NIST (National Institute of Standards and Technology) standards. The engine lubricants were chosen among the most common mixtures and compounds used in automotive engines, for instance, the oils VM1 and VM2 refer to fully formulated engine lubricants with two different viscosity modifiers while the Detergents refer to oils with different TBN (total base number). The viscosity of all the oils has been measured with a cone viscometer at $10^2\ s^{-1}$ at three temperatures.

| Oil Type | Oil Sample | Viscosity (Pas) @25 °C | Viscosity (Pas) @40 °C | Viscosity (Pas) @50 °C |
|---|---|---|---|---|
| Mineral Oils | S20 | 0.029 | 0.015 | 0.010 |
| | N35 | 0.055 | 0.027 | 0.018 |
| | N100 | 0.200 | 0.083 | 0.050 |
| | S200 | 0.407 | 0.155 | 0.092 |
| | S600 | 1.329 | 0.446 | 0.240 |
| Synthetic Oils | PAO 8 | 0.089 | 0.043 | 0.031 |
| | PAO 40 | 0.914 | 0.349 | 0.231 |
| | PAO 100 | 3.540 | 1.218 | 0.765 |
| Fully Formulated Engine Oils | VM1 | 0.246 | 0.102 | 0.071 |
| | VM2 | 0.118 | 0.057 | 0.041 |
| | High Detergent | 0.084 | 0.041 | 0.031 |
| | Low Detergent | 0.116 | 0.051 | 0.036 |
| | Ester | 0.234 | 0.099 | 0.069 |

**Table 1: Samples tested and the viscosities measured with a cone viscometer at a shear rate of $\mathbf{10^2\ s^{-1}}$**

## 5. Signal processing and data analysis.

Initially the frequency dependent reflected amplitude spectrum $A_r(f)$ is derived when there is no oil present. Since almost all the wave is reflected back non-attenuated at an air interface, this signal is equal to the incident signal and serves as a reference. All subsequent measurements from solid-liquid interfaces, $A_m(f)$, are divided by this reference to give the reflection coefficient, *R*. The pulsing signal employed is a chirp as shown in Figure (8). This is a signal modulated in frequency; which means that with a single chirp burst it is possible to excite a range of different frequencies.

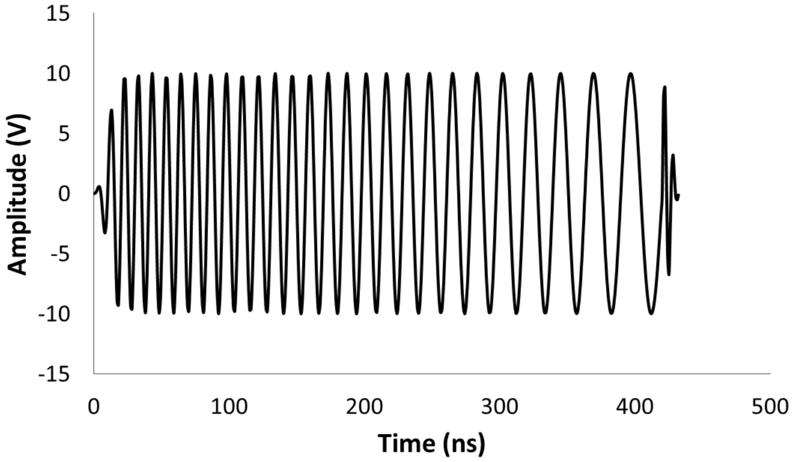

**Figure 8: Chirp pulse 3-10 MHz, time domain representation.**

The chirp is used because it ensures that the exact frequency at which matching layer resonance is included in the bandwidth. Figure (9a) shows the applicable frequency spectrum of the reflected pulse when there is a fluid sample in a contact and when it is absent.

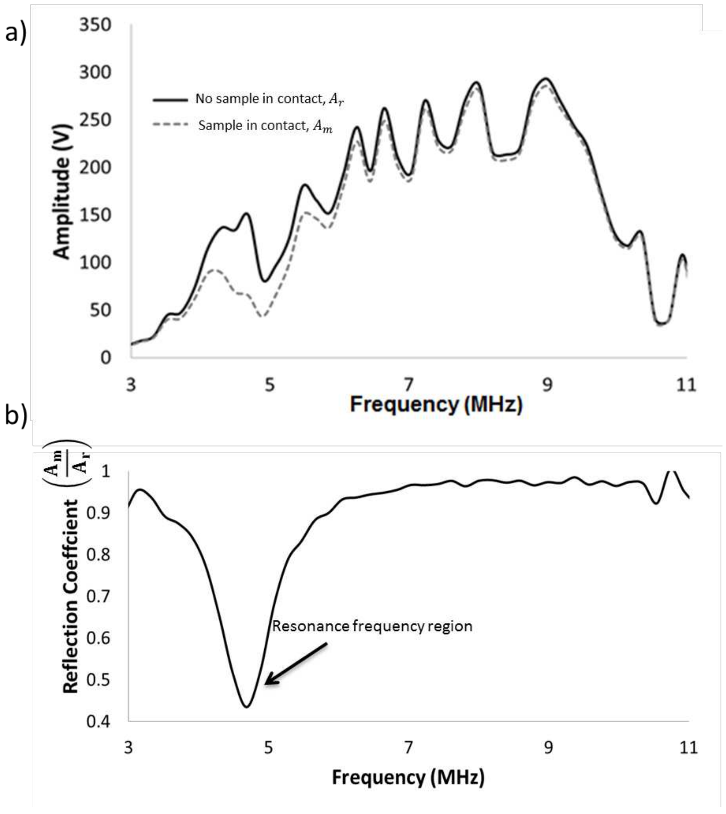

**Figure 9: a) Chirp FFT for measurement and calibration reference. b) Reflection coefficient: it is highlighted the increment in sensitivity at the resonance frequency, while outside resonance the reflection coefficient approaches 1.**

Figure (9b) shows the reflection coefficient spectrum calculated by dividing the amplitude of the measurement (signal from solid-oil interface) by the reference measurement (acquisition at solid-air interface):

$$R = \frac{A_m}{A_r} \tag{15}$$

The presence of the matching layer causes resonance, and so a drop in the reflection coefficient, to occur between 4.0 and 6.0 MHz. The maximum drop in reflection coefficient occurs at 4.5 MHz and this is the value of reflection coefficient used in the viscosity measurement.

# 6 Results

## 6.1 Measurement sensitivity increment

Figure (10) shows the reflection coefficient obtained over a range of frequencies for a series of mono- and multi-grade lubricant oils. The effect of the matching layer is evident from the reflection response; resonance frequencies are observed at 4.5 MHz and 14.5 MHz. Further resonances would occur at higher frequencies, as stated in equation (9), but these are outside the bandwidth of the transducers used.

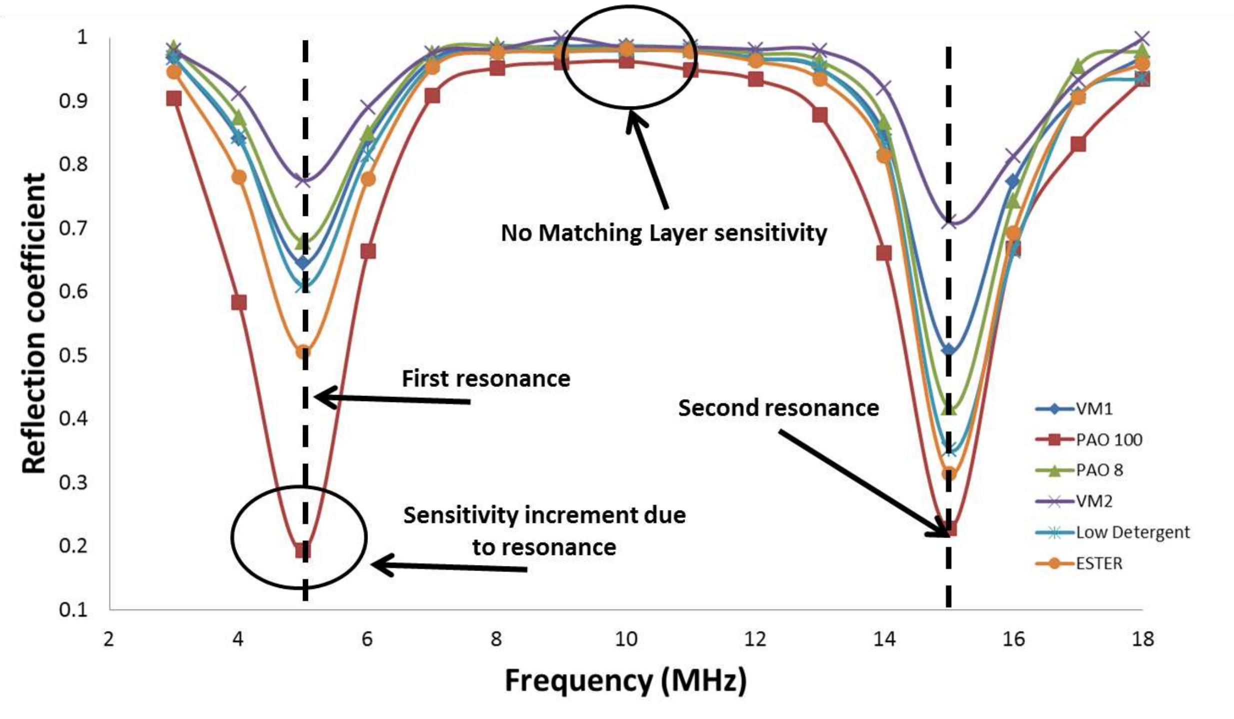

Figure 10: Sensitivity increment at resonance.

At the resonance frequencies the response of the different lubricant viscosities is well separated. Away from the resonance frequency, for example at 10 MHz, all the lubricant films show a reflection close to one and it is hard to discriminate between them. This figure shows the importance of the matching layer technique. Without the matching layer the response would be similar to that which occurs at 10 MHz across the whole frequency spectrum. Table 2 reports the reflection coefficient at the first resonance frequency, 4.5 MHz, and away from resonance, at 10 MHz. The reported values are obtained from the mean of five experimental repetitions.

| Frequency (MHz) | Sample | Mean Reflection coefficient | Standard Deviation |
|---|---|---|---|
| 4.5 | VM1 | 0.634 | 0.011 |
|  | VM2 | 0.784 | 0.011 |
|  | PAO 8 | 0.687 | 0.013 |
|  | PAO 100 | 0.200 | 0.015 |
|  | High Detergent | 0.607 | 0.020 |
|  | ESTER | 0.515 | 0.012 |
| 10 | VM1 | 0.986 | 0.012 |
|  | VM2 | 0.984 | 0.014 |
|  | PAO 8 | 0.983 | 0.015 |
|  | PAO 100 | 0.962 | 0.015 |
|  | High Detergent | 0.979 | 0.017 |
|  | ESTER | 0.981 | 0.018 |

**Table 2. Sensitivity increment at resonance**

The table shows that the matching layer technique does not improve the accuracy of the ultrasound method, but increases the sensitivity to fluid viscosity. The standard deviation in the reflection coefficient is in fact equivalent to around 1% for both the cases, but in the case of resonance an error of ±1% is acceptable, while outside resonance the same error makes it impossible to distinguish between different samples.

## 6.2 Viscosity results for Newtonian oils

Figure (11) shows the reflection coefficients acquired for a set of calibrated mineral oils around the resonance frequency. The mineral oils were chosen for their Newtonian behaviour thus being ideal to test the efficiency of the ultrasonic viscometer.

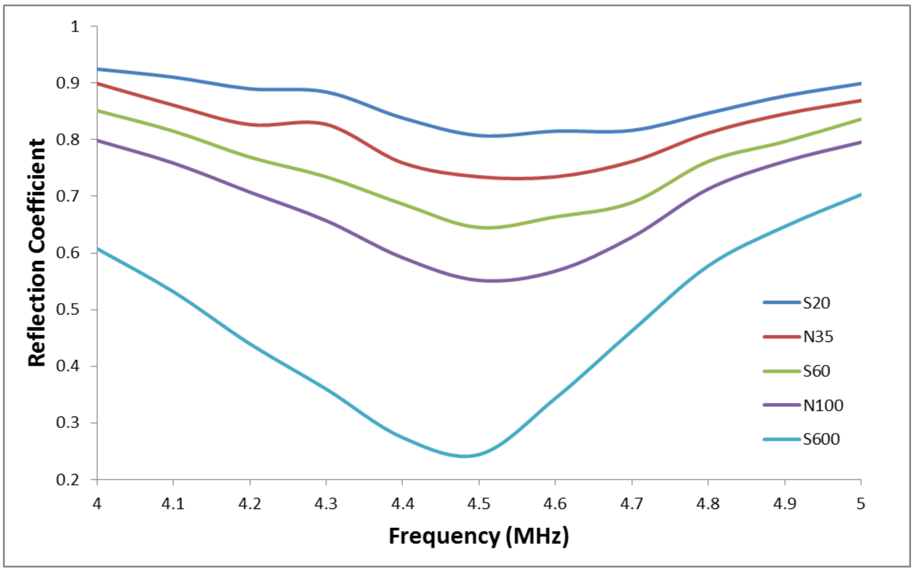

**Figure 11: Reflection coefficient at resonance for calibrated Newtonian oils.**

The reflection coefficient values at 4.5 MHz were used in equation (8) to obtain the oil viscosity. Figure (12) shows viscosities measured with the ultrasonic method plotted against the viscosity determined using a conventional cone viscometer. This plot shows the excellent agreement between the predicted and measured data with a correlation coefficient of $R^2$=0.999.

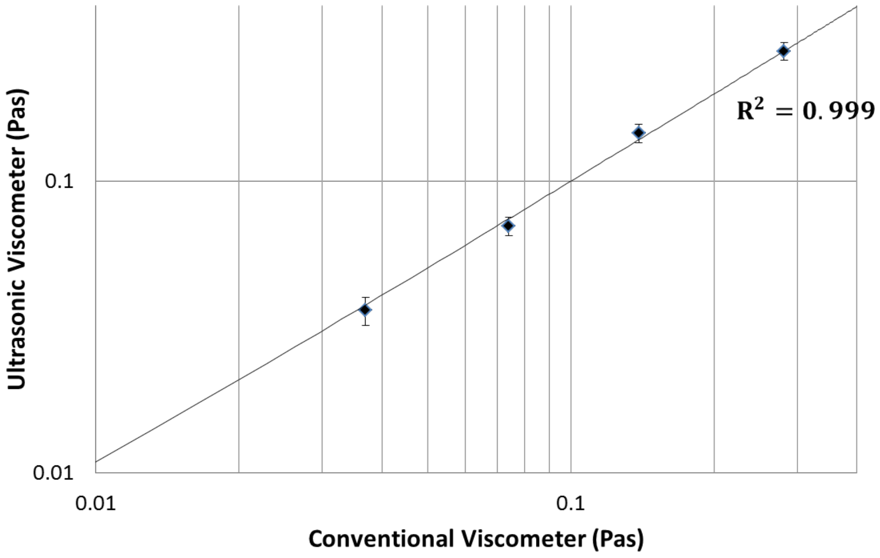

Figure 12: Ultrasonic viscometer versus conventional cone viscometer plot.

Figure (13) shows the reflection coefficient plotted against the viscosity values measured with a conventional cone viscometer for the tested mineral oils. The Maxwell model of reflection given as equation (8) is also plotted; the results are in good agreement.

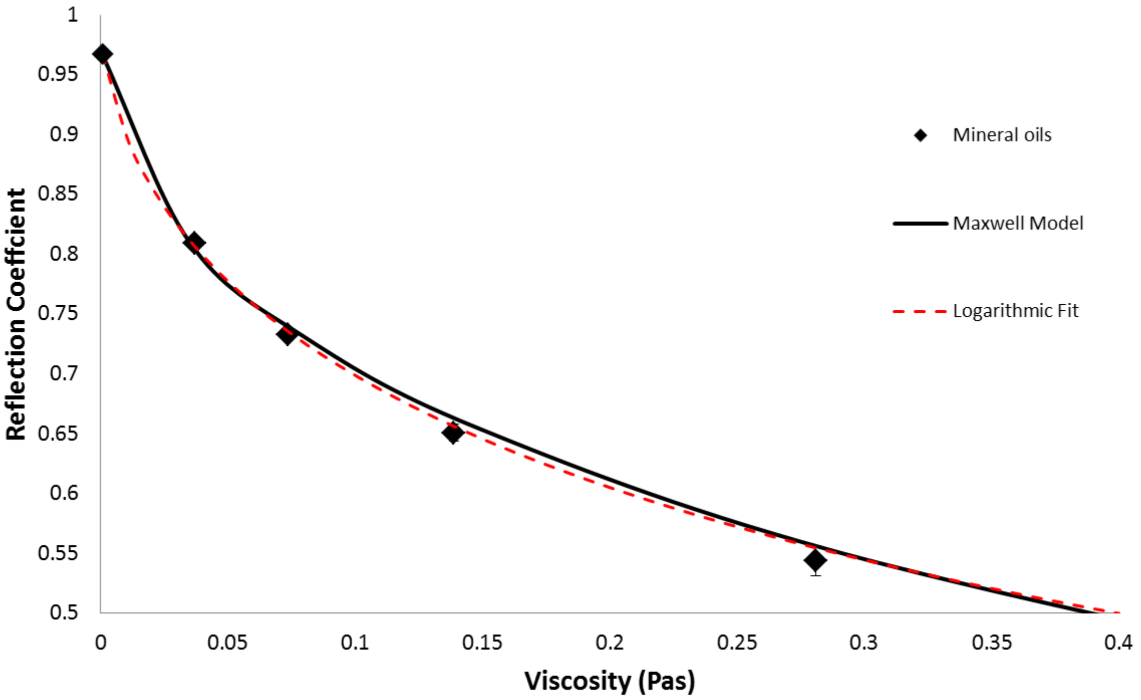

Figure 13: Relationship between reflection coefficient and viscosity for standard mineral oils. The experimental data respect the Maxwell model and a logarithmic fit.

The Maxwell model, equation (8), contains some parameters, like fluid density and the oil acoustic impedance, that need to be measured in order to convert *R* to viscosity. Another approach for determining the relationship between viscosity and reflection coefficient would be to calibrate a particular list of known viscosity Newtonian oils by curve fitting the pairs of ($\eta$,$R$) experimental data points. A logarithmic relation fit to the data points is also shown on Figure (13):

$$\eta = a_2 e^{-\left(a_3\sqrt{\frac{ln\,(R-a_0)}{a_1}}\right)} \tag{16}$$

Where the coefficients of equations (16) have the following values:

| Coefficient | Value |
|---|---|
| $a_0$ | 0.98305 |
| $a_1$ | -0.92349 |
| $a_2$ | 21.198 |
| $a_3$ | 4.9335 |

**Table 3: Coefficient of the logarithmic fit function, equation (16)**

This type of empirical law does not need the prior knowledge of any fluid properties to determine the viscosity, but only the measured reflection coefficient. It is then a useful tool to interpret the data acquired by an ultrasonic viscometer working in-situ.

### 6.3 Viscosity results for fully formulated engine lubricants

The reflection coefficient data for the formulated engine lubricants reported in Table (2) were converted into viscosity using equation (14). Figure (14) reports the comparison of the viscosity measured with the ultrasonic method for fully formulated engine lubricants against the viscosity measured with a cone viscometer at $10^2$ $s^{-1}$.

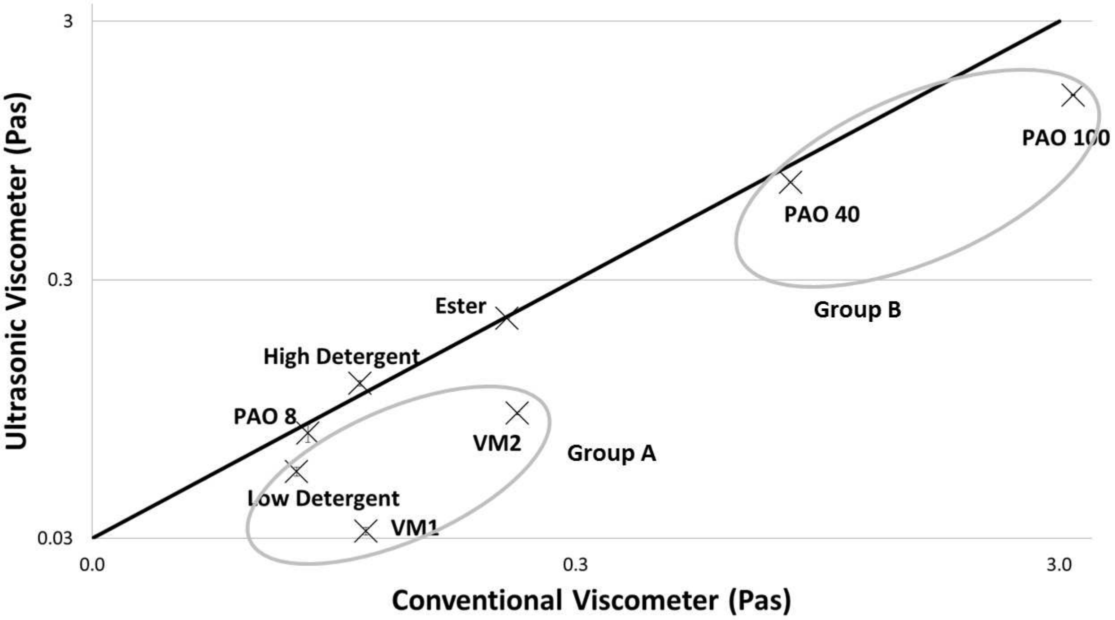

**Figure 14: Ultrasonic viscometer versus conventional cone viscometer plot, comparison among Newtonian sample and engine lubricants.**

Figure (14) shows that for certain oils, the ultrasonic measurement deviates from the conventional cone viscometer results. The oils indicated as Group A in Figure (14) highlight that as the molecular structure of the oil gets more complex the deviation from the viscosity values measured with the cone rheometer increases, and more precisely, this deviation looks like a shear thinning behaviour. The reason for the shear thinning of the ultrasonic results is due to the composition of the oil and the shear rate excited at the solid-oil contact interface. Engine lubricants consist of a base oil (mineral or synthetic) plus a concentration of additives (polymer or not). This structure responds differently to a mechanical shear and to an oscillatory shear as schematically shown in Figure (15). A common viscometer shears the whole fluid sample and for high values of the shear rate aligns the polymer chains thus leading to an expected shear thinning effect that is a function of the response of both polymer and base. For the oscillatory case, a high frequency ultrasonic shear wave travels through the sample for a very short distance. In this case the shear rate excited (4.5 MHz) is such that the oscillation of the solid-oil boundary is too fast to match the polymer relaxation time (order of magnitude $10^5$ $s^{-1}$). When the ultrasonic wave strikes the oil boundary the high inertia particles oscillate, but they respond fast enough to influence the reflection of the ultrasonic wave. Therefore only the simpler molecular structure base oil influences the ultrasonic measurement.

A similar phenomenon happens for the PAO samples, indicated as Group B on figure 14. It is possible to notice that PAO8, the PAO with the lower molecular weight, shows a Newtonian behaviour, while as the PAO molecular weight increases the deviation from the cone viscometer results increase. The shear thinning behaviour for this class of oils is then associated with the increment in molecular weight because at high frequencies the PAO molecules tend to pack up and oscillate together thus reducing the apparent viscosity.

The viscosities of the group B samples have been extensively studied over a wide range of shear rates to measure EHL film thickness by means of steady shear viscometers [17, 18]. A unified theory has not been developed yet to correlate the steady shear viscosity and the oscillatory viscosity at high shear rate. In any event, it is instructive to compare the results obtained with the ultrasonic viscometer proposed in this work, with published methodologies. Bair et al. [17] compares steady shear viscosity at low and high shear rate using the modified Carreau equation, through the relationship:

$$\eta(\omega) = \mu \sum_{i=1}^{N} x_i \left[1 + \left(\frac{\tau}{G_i}\right)^2\right]^{(1-1/n_i)/2} \tag{17}$$

Where $\eta$ is the viscosity at high shear stress, $\mu$ is the viscosity at low shear stress, $\tau$ is the shear stress at the strain rate at which viscosity is measured, $G$ is the effective shear modulus, $x$ and $n$ are constants in the model obtained empirically for each oil. Here, the same approach is implemented for the oscillatory case, replacing $\tau$ by $\mu\omega$, as done by Bair et al. [19]. Application of equation (17) to the ultrasonic viscometer reading gives the results listed in Table 4.

| Oil | $\mu$ low shear rate viscosity(Pas) | $\eta$ modified Carreau @ 4.5 MHz (Pas) | $\eta$ ultrasound (Pas) @ 4.5 MHz | Deviation(%) |
|---|---|---|---|---|
| PAO 40 | 0.914 | 0.657 | 0.715 | 8.2% |
| PAO 100 | 3.201 | 1.33 | 1.47 | 9.5% |

**Table 4: Comparison of the ultrasonic results with the Bair model for the PAO samples. The low shear viscosity was obtained from a conventional viscometer; this value was used in equation (17) to predict a high shear value; which is subsequently compared to the ultrasonic high shear value.**

The agreement with the ultrasonic data and that predicated by the modified Carreau model is reasonable for both oils. This is encouraging given there are a number of inherent assumptions.

Firstly, the constants *x* and *n* in equation (17) were derived for PAO40 and 100 under steady shear rather than the lower pressure and oscillatory shear of the present work. Secondly, the PAO blends analysed are slightly different. Thirdly, the constants were derived for conditions of high pressure because shear cavitation occurred at atmospheric pressure. Finally, it is supposed that the vibrational frequency in the oscillatory viscometer is equivalent to the shear rate at steady shear. This approximation is not satisfactory at high shear rates, as it is discussed in further details in Section 6.4.

The lubricants that are not highlighted in either groups A or B show Newtonian behaviour. These lubricants do not appear to show any dependency of the viscosity upon the shear rate and the reading of the ultrasonic viscometer matches that of the cone viscometer.

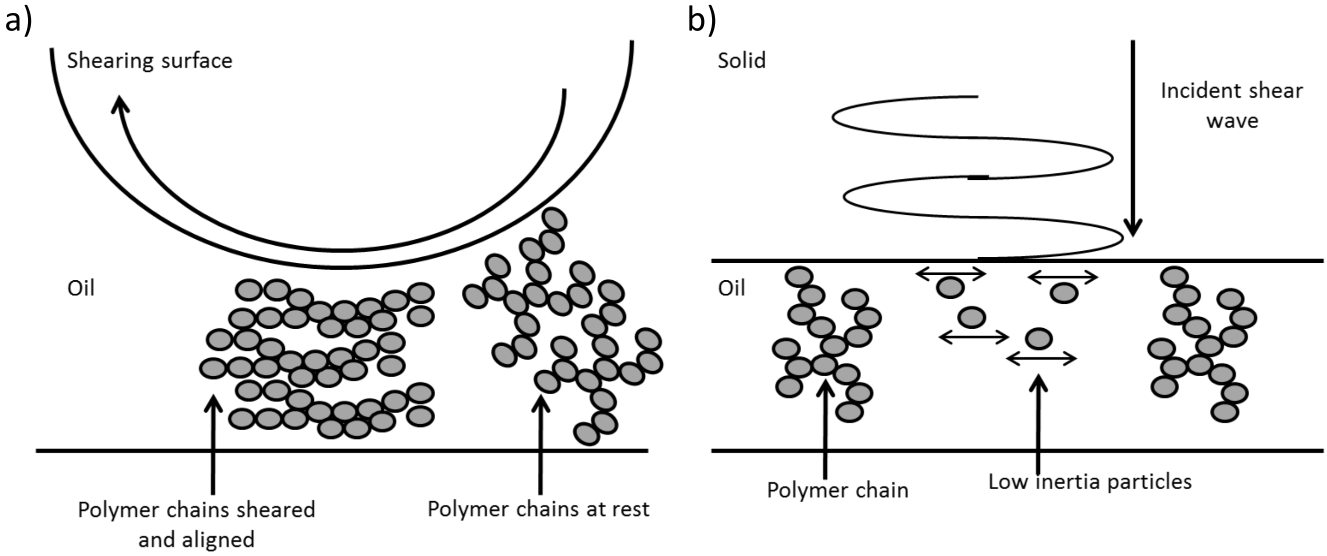

**Figure 15: (a) Effect of rotational viscometer on polymer chains. At high rotational speed the polymer chains are aligned thus reducing the apparent viscosity. (b) High frequency shear wave incident to solid-oil boundary. Only the low molecular weight particles affect the viscosity measurement.**

## 6.4 Effect of polymer concentration and excitation frequency

Several researchers have compared viscosity from an oscillatory shear and a mechanical induced steady shear [20, 21, 22]. Cox and Merz [20] introduced a generally accepted empirical rule to compare the shear strain of conventional viscometers and oscillatory based ones:

$$\eta(\omega) = \eta(\dot{\gamma})|_{\dot{\gamma}=\omega} \tag{18}$$

Where $\dot{\gamma}$ is the shear strain from a conventional rotational viscometer. This rule states that the rotational frequency of an oscillatory based viscometer is equal to the shear strain at the solid-liquid boundary and that the measurement made with such a technique is comparable with the reading from a conventional rheometer. This rule has been validated for rotational frequencies up to $10^4$ Hz [23]. At high shear rates this is no longer, especially for polymer based oils. Larson [24] states of the viscosity measurement executed with an oscillatory technique on a polymer oil: "*In the bead and spring description, a polymer molecule contributes nothing to the viscous dissipation if the deformation is too fast. In this limit, the dilute solution acts as a suspension of rigid particles, and the viscosity is constant*". Bair [19] experimentally explored the Cox-Merz rule at high rotational frequencies ($10^7$ Hz), with different base oils, using an impedance spectrometer microbalance and discovered that this rule was no longer valid. The matching layer ultrasound viscometer results in section 6.3 also show the same behaviour for the polymer based oils. This can be seen by comparing measurements at a shear rate of 4.5 MHz both with an ultra-high shear viscometer (UHSV) and with the proposed ultrasonic viscometer on different mixtures with the same base oil and different polymer concentrations. Table (5) reports the mixture polymer content and viscosity measured with both the UHSV and the ultrasonic viscometer at 4.5 MHz at 100 °C.

| Sample | Base (%) | Polymer concentration (%) | Viscosity (Pas) @100 °C [UHSV,4.5 Mc/s] | Viscosity (Pas) @100 °C [Ultrasound,4.5 Mc/s] |
|---|---|---|---|---|
| Base 1 | 100 | 0.0 | 0.00618 | 0.00611 |
| Mixture 1 | 99.5 | 0.5 | 0.00673 | 0.00620 |
| Mixture 2 | 99.0 | 1.0 | 0.00772 | 0.00616 |
| Mixture 3 | 98.0 | 2.0 | 0.01243 | 0.00629 |

**Table 5: Polymer concentration and viscosity of several custom mixtures**

Figure (16) shows that the viscosity measured with ultrasound is independent of the polymer concentration and is coincident with the base viscosity (0% polymer concentration). These results demonstrate that the lubricants are sheared too quickly to match the relaxation time of the polymer. In order to obtain the viscosity value for a complex fluid it is then necessary to reduce the interface shear stress by reducing the transducer frequency.

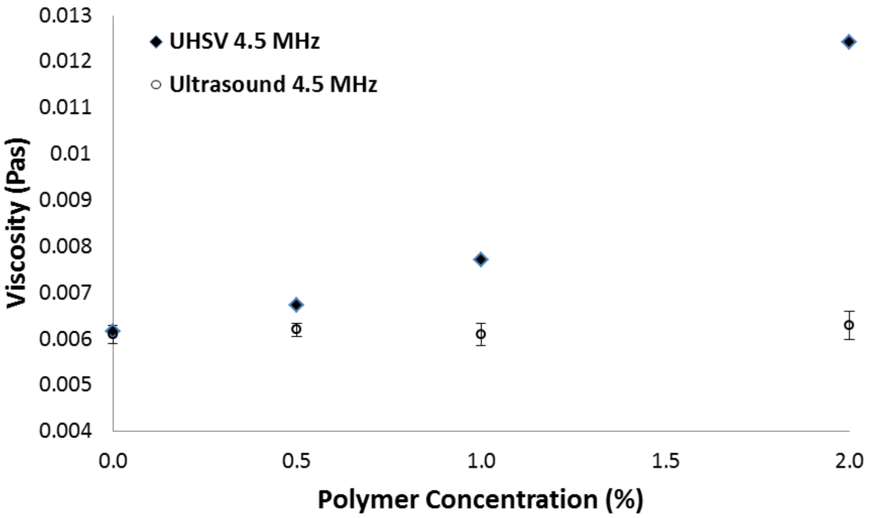

**Figure 16: Polymer concentration against viscosity measured at different shear rates for custom mixtures @ 100 °C.**

## 7 Conclusions

This work proposes a novel ultrasonic viscometer based on the use of a matching layer to improve coupling of ultrasound between a metal bearing and an oil sample. This approach significantly improves measurement sensitivity at a solid-liquid boundary making viscosity measurements extremely precise. Because the matching layer method allows good coupling between a metal and a liquid, it has the potential to be further developed for in-situ applications in engine components.

Oils with different Newtonian and Non-Newtonian characteristics have been tested with the ultrasonic viscometer and the results compared with a standard cone viscometer and with an ultra-high shear viscometer. The results show perfect agreement between the viscosity measured for Newtonian oils with conventional viscometers and the data acquired by the ultrasonic viscometer. However for Non-Newtonian oils, the study has highlighted a dependency between the shear rate induced at the contact interface by ultrasonic waves and the lubricant polymer particle relaxation time. In particular, it is noted that at MHz frequencies only the base of the lubricant is sheared, thus excluding the polymer effect from the ultrasound response.

## References

1. Mason, W.P.: Measurement of shear elasticity and viscosity of liquids at ultrasonic frequencies*.,* Physical Review, 7S, 936-946 (1949)
2. Roth, W.: A New Method for Continuous Viscosity Measurement. General Theory of the Ultra-Viscoson*.,* Journal of Applied Physics, 24, 940-950 (1953)
3. Cohen-Tenoudji, F., Ahlberg, L.A., Tittmann, B.R. et al.: High temperature ultrasonic viscometer*.* Patent No.: 4,779,452, USA (1988)
4. Sheen, S.H., Lawrence, W.P., Chien, H.T. et al.: Method for measuring liquid viscosity and ultrasonic viscometer*.* Patent No: 5,365,778, USA (1994)
5. Hinrichs, R.J., Thuen, J.: Method for Determining Resin Viscosity with Ultrasonic Waves., Patent Number 4,559,810, USA (1985)
6. Shah, V., Balasubramaniam, K.: Effect of viscosity on ultrasound wave reflection from a solid/liquid interface, Ultrasonics, 34 (8), 817-824 (1996)
7. Buiochi, F., Higuti, R.T., Furukawa, C.M. et al.: Ultrasonic measurements of viscosity of liquids, Ultrasonics Symposium, 1, 525-528 (2000)
8. Behrends, R., Kaatze, U.: A high frequency shear wave spectrometer for low viscosity liquids, Measurement Science and Technology, 12(4), 519 (2001)
9. Barlow, A.J., Lamb, J.: The Visco-elastic behaviour of Lubricating oils under cyclic shearing stress*.,* Proceedings of the Royal Society A Mathematical Physical and Engineering Sciences, 253(1272), 52-69 (1959)
10. Lamb, J.: Physical properties of fluid lubricants: rheological and viscoelastic behaviour*.,* Proceedings of the Institution of Mechanical Engineers, Conference Proceedings, 182:293 (1967)
11. Harrison, G., Barlow, A.J.: Method of Experimental Physics, Ultrasonics, Academic Press, 19(3) (1981)
12. Franco, E.E., Adamowski, J.C., Higuti, R.T. et al. Viscosity measurement of Newtonian liquids using the complex reflection coefficient*.,* IEEE Transactions on Ultrasonics, Ferroelectrics, and Frequency Control, 55 (10), (2008)
13. Schirru, M.M., Dwyer-Joyce, R.S.: A model for the reflection of shear ultrasonic waves at a thin liquid film and its application to viscometry in a journal bearing, Proceedings of the Institution of Mechanical Engineers, Part J: Journal of Engineering Tribology, [online] (2015)
14. Buckin, V., Kudryashov, E.: Ultrasonic shear wave rheology of weak particle gels., Advances in colloid and Interface Science, 89-90, 401-422 (2001)

15. Alvarez-Arenas, T.G.: Acoustic impedance matching of piezoelectric transducers to the air., IEEE Transactions on Ultrasonics, Ferroelectrics, and Frequency control, 51(5) (2004)
16. Kinsler, L., Frey, A., Coppens, A. et al.: Fundamentals of Acoustics Wiley, Fourth Edition, New York (1999)
17. Bair, S., Vergne, P., Querry, M.,: A unified shear-thinning treatment of both film thickness and traction in EHD., Tribology Letters, 18(2), 145-152 (2005)
18. Bair, S., Liu, Y., Krupka, I., et al.: The shear-thinning elastohydrodynamic film thickness of a two-component mixture., Journal of Tribology, 130(2), 021502(2008)
19. Bair, S., Yamaguchi, T., Brouwer, L., Schwarze,H., et al.: Oscillatory and steady shear viscosity: The Cox-Merz rule superposition and application to EHL friction, Tribology International, 79, 126-131 (2014)
20. Cox, W.P., Merz, E.H.: Correlation of dynamic and steady flow viscosities., Journal of Polymer Science, 28(118), 619–22 (2003)
21. Al-Hadithi, T.S.R., Barnes, H.A., Walters, K.: The relationship between the linear (oscillatory) and nonlinear (steady-state) flow properties of a series of polymer and colloidal systems., Colloid and Polymer Science, 270, 40 (1992).
22. Laun, H.M.: Prediction of elastic strains of polymer melts in shear and elongation., Journal of Rheology, 30, 459-501 (1986)
23. Dealy, J.M., Larson, R.G.: Structure and rheology of molten polymers, Hanser, Chicago (2006)
24. Larson, R.G.: Constitutive equations for polymer melts and solutions, Butterworths, Boston (1988)